Predictability of Tropical Pacific Decadal Variability in an Intermediate Model*

ALICIA R. KARSPECK, RICHARD SEAGER, AND MARK A. CANE

Lamont-Doherty Earth Observatory, Columbia University, Palisades, New York

(Manuscript received 17 September 2003, in final form 16 February 2004)

ABSTRACT

The Zebiak–Cane (ZC) model for simulation of the El Niño–Southern Oscillation is shown to be capable of producing sequences of variability that exhibit shifts in the time-mean state of the eastern equatorial Pacific that resemble observations of tropical Pacific decadal variability. The model's performance in predicting these shifts is compared to two naive forecasting strategies. It is found that the ZC model consistently outperforms the two naive forecasts that serve as a null hypothesis in assessing the significance of results. Forecasts initialized during anomalously warm and anomalously cold decades are shown to have the highest predictability.

These modeling results suggest that, to a moderate extent, the state of the tropical Pacific in one decade can predetermine its time-mean state in the following decade. However, even in this idealized context decadal forecasting skill is modest. Results are discussed in the context of their implications for the ongoing debate over the origin of decadal variations in the Pacific.

1. Introduction

Pacific decadal variability

Decadal-scale variability in the tropical and North Pacific Ocean has been documented and analyzed using both observations and modeling studies (e.g., Trenberth and Hurrell 1994; Graham 1994; Miller et al. 1994a,b; Zhang et al. 1997; Guilderson and Schrag 1998; Miller and Schneider 2000; Karspeck and Cane 2002; Seager et al. 2004). Much of this work has focused on the shift toward warmer tropical sea surface temperatures and cooler North Pacific sea surface temperatures that occurred in 1976. But there are other examples of ''shifts'' in the observational record, such as the 1943 shift toward cooler conditions in the tropical Pacific (Zhang et al. 1997). These have received less attention, at least partially due to the paucity of observational data available for the Pacific prior to the late 1970s. Observations of tropical Pacific sea surface temperatures (SSTs) also suggest that the descent into a La Niña following the 1997–98 El Niño marked another shift in the climate of the Pacific, although it is impossible to foretell how long these cool conditions will endure. A number of terms have been coined to describe these long-term climate fluctuations [e.g., the Pacific decadal oscillation (PDO), the North Pacific Oscillation, decadal–ENSO variability]. In this study, we will use the more general term Pacific decadal variability (PDV). PDV has important implications for the North American climate (Latif and Barnett 1996) and fisheries productivity off the coast of Alaska and the northwestern United States (e.g., Mantua et al. 1997; Hare et al. 1999).

Although the evidence for these climatic shifts is plentiful and a variety of mechanisms have been proposed, there does not yet exist a coherent theory that explains the generation or maintenance of the variability; nor is there a clear understanding of the relative (and possibly interactive) roles of the Tropics and the higher latitudes. The existing literature has tended to focus on mechanisms that favor an active role of the midlatitudes in generating anomalies (e.g., Latif and Barnett 1996; Gu and Philander 1997; Vimont et al. 2001). Under this paradigm, conditions in the North Pacific—which could be generated as a remote response to tropical forcing or through internal variability—are communicated to the Tropics via an oceanic or atmospheric bridge. The Tropics are posited to respond to these remotely generated anomalies through modulation of the ENSO cycle.

However, PDV that originates and is maintained within the tropical Pacific remains a viable hypothesis. The delayed oscillator mechanism (Battisti 1988; Suarez and Schopf 1988), typically used to explain interannual ENSO, can produce variability at decadal periods (Chang et al. 1995; Knutson and Manabe 1998). Timmermann and Jin (2002) argue that tropical ocean–at-

* Lamont-Doherty Earth Observatory Contribution Number 6592.

Corresponding author address: Dr. Alicia R. Karspeck, Lamont-Doherty Earth Observatory, Columbia University, 301F Oceanography, Box 1000, Palisades, NY 10964.
E-mail: aliciak@ldeo.columbia.edu

mosphere interactions can modulate the amplitude of the ENSO cycle on decadal time scales. Nonaka et al. (2002) suggest that modulation of the strength of the subtropical overturning cell can be driven by off-equatorial zonal wind anomalies.

Regardless of the mechanism, decadal variability in the Tropics can then remotely affect the high latitudes through the same atmospheric teleconnections that operate on interannual time scales (Lau and Nath 1996; Lau 1997). Modeling results from Alexander et al. (2002) suggest that one-quarter to one-half of the variance of the dominant pattern of low-frequency variability in the North Pacific arises from tropical forcing via the ''atmospheric bridge'' (Alexander 1992).

Invoking hypotheses of high-latitude origin have the attractive by-product of introducing a characteristic anomaly evolution that operates on time scales on the order of decades (Latif and Barnett 1996). If midlatitude-generated anomalies are assumed to take an oceanic path to the Tropics, then there is a travel time from inception to tropical amplification on the order of a decade (Gu and Philander 1997). This suggests that with a proper understanding and observation of the system, it would be possible to predict these climate fluctuations years in advance (Latif 1998).

But if PDV originates in the Tropics—where the climate signal is dominated by interannual variability and the coupled system is possibly chaotic—is prediction of decadal variability possible?

To help elucidate the question of PDV origin, it would be desirable to determine if the trigger for an abrupt shift in the phase of the PDV is present in the tropical Pacific in the years prior to a shift. In other words, does the state of the tropical Pacific in one decade predetermine its time-mean state in the following decade?

Unfortunately, the shortness of the observational record limits our ability to address this question using data alone. There are only a small number of ''shifts'' in the time-mean state evident in the observational record. In this study, then, we use a synthetic record that contains many examples of decadal scale shifts, which was generated by the Zebiak–Cane (ZC) model of the tropical Pacific ENSO system. As we will show, the model is capable of producing time sequences of tropical variability that exhibit shiftlike behavior similar to the handful that have been observed.

We then address whether the shifts in these modeled sequences are predictable by the tropical-only ENSO model some years in advance. Which is to say, are there coherent structures in the tropical ocean–atmosphere that signal a coming shift in the time-mean state of the system? The result will most likely be an overestimate—an upper bound on the predictability of the real Pacific: It neglects all connectivity with higher latitudes as well as higher frequency tropical noise.

Section 2 introduces the intermediate coupled ENSO model and the observational data used in this study. Section 3 presents assessments of the predictability of time-mean shifts of the tropical climate using the model. Sections 4 and 5 compare the model's predictability with two naive forecasting strategies (null hypothesis). Section 6 concludes our findings.

2. Description of model and observational data

The model we use is an intermediate coupled model of the El Niño–Southern Oscillation (ENSO) described in Zebiak and Cane (1987). The ZC model was integrated for 150 000 yr. The average SST anomaly in the Niño-3 region (5°S–5°N, 150°–90°W) was retained at monthly intervals, yielding a time series of 1.8×10^6 months in length. This model series will henceforth be referred to as ''ZC-Long.''

Observations of the average SST anomaly in the Niño-3 region were computed from the Kaplan optimal analysis of MOHSST5 SST anomalies (Kaplan et al. 1998) every month from January 1856 to December 1991. We will refer to this series as ''Kaplan SST.''

3. Predictability of shifts in the 15-yr mean of the Niño-3 index

From the Kaplan SST, we found three 30-yr segments that exhibit shifts in the timemean of the two adjacent 15-yr periods: a positive, negative, and neutral shift. The size of the shift is defined as the difference in means between the second and the first 15-yr period. The positive and negative shifting segments were chosen because they have shifts of the greatest magnitude in the Kaplan SST record. The segment corresponding to the neutral shift was chosen because it had a shift size closest to zero. Figure 1 shows the *warm shift* segment (hereafter referred to as ''W-obs''; centered at January 1976), the *neutral shift* segment (hereafter referred to as ''N-obs''; centered at January 1903), and the *cold shift* segment (hereafter referred to as ''C-obs''; centered at January 1943). The segments that shift toward colder/warmer means each show an absolute difference in means greater than 0.3°C. The segment with no shift (N-obs) shows an absolute difference of less than 0.1°C.

We then searched ZC-Long for the 30-yr segments that had the highest correlation with the observed segments, C-obs, W-obs, and N-obs, and had appropriately sized shifts in the mean (absolute value of more than 0.3°C for warm and cold shifting segments and less than $\pm$0.1°C for neutral shifting segments). Twenty-four instances (we will refer to these segments as ''analogs'') for each of the three observed segments were retained (totaling 72). Figure 1 shows the model analogs with the highest correlation to C-obs, W-obs, and N-obs. (Correlation and shift size for all 72 model instances are shown in Table 1.)

There are 93, 10, and 16 analog segments that correlate with W-obs, N-obs, and C-obs, respectively, at an R value greater than 0.5. This means that 30-yr segments that match the observed shifts occur in the ZC model

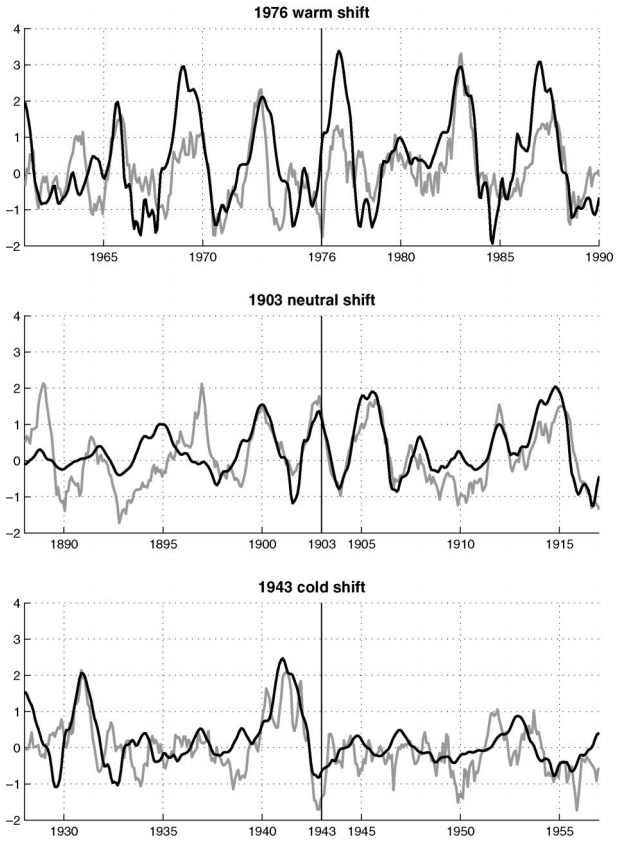

FIG. 1. Observed Niño-3 averaged SST anomalies (gray line) taken from Kaplan et al. (1998). A 30-yr segment of Niño-3 SST anomaly (blackline) from ZC-Long (150 000-yr integration of ZC model) with the highest correlation. Correlation values are in Table 1. Observed shifts in Niño-3 SSTA between first and second 15-yr segments are 0.35°C for 1976 warm shift, −0.09°C for the 1903 neutral shift, and −0.33°C for the 1943 cold shift.

about once every 1600 yr for warm shifts, once every 15 000 yr for neutral shifts, and once every 9300 yr for cold shifts.

The spatial patterns of warm and cool decadal shifts produced by this model are similar to its interannual ENSO pattern. The maximum is centered on the equator within the Niño-3 region and is meridionally narrow. The SST anomaly difference patterns in the observed warm and cool decadal shifts is qualitatively similar, but with a more meridionally broad signal. The observed 1976 warm shift has an additional maximum just west of the date line, although the 1943 warm shift does not. The absence of the broad structure in the model decadal shifts could be attributed to insufficient communication between the mixed layer and the thermocline or the neglect of other terms such as wind speed and cloud-cover variations in the model net surface heat flux. Hazeleger et al. (2004) show that the meridional breadth of the decadal ENSO pattern can also be affected by variations in the strength of the Indonesian Throughflow, which varies in response to the phase of ENSO. This process is not resolved in our intermediate model.

TABLE 1. The correlation coefficients (R) between W-obs, N-obs, and C-obs, and the 30-yr model-generated analog segments (from ZC-Long). Also, the size (in °C) of the difference in the means of the second and first 15-yr segments of the analog.

	Warm shift		Neutral shift		Cold shift	
	R	Shift size	R	Shift size	R	Shift size
1	0.64	0.41	0.63	0.09	0.59	−0.36
2	0.64	0.37	0.58	−0.06	0.56	−0.39
3	0.63	0.48	0.57	0.07	0.56	−0.37
4	0.63	0.36	0.56	−0.06	0.55	−0.33
5	0.62	0.30	0.55	−0.06	0.55	−0.32
6	0.61	0.43	0.54	0.03	0.54	−0.31
7	0.61	0.38	0.53	−0.03	0.54	−0.54
8	0.61	0.31	0.53	0.01	0.54	−0.59
9	0.60	0.32	0.51	0.02	0.54	−0.40
10	0.59	0.39	0.50	−0.002	0.54	−0.49
11	0.59	0.36	0.50	0.05	0.53	−0.31
12	0.58	0.45	0.50	0.04	0.53	−0.42
13	0.58	0.47	0.49	−0.08	0.53	−0.45
14	0.58	0.51	0.49	−0.06	0.52	−0.41
15	0.58	0.48	0.49	−0.09	0.51	−0.64
16	0.58	0.37	0.49	−0.07	0.50	−0.51
17	0.58	0.39	0.48	0.04	0.50	−0.37
18	0.58	0.40	0.48	−0.07	0.50	−0.32
19	0.57	0.40	0.49	−0.05	0.50	−0.33
20	0.57	0.36	0.48	−0.06	0.50	−0.40
21	0.57	0.44	0.47	−0.04	0.50	−0.36
22	0.56	0.43	0.47	−0.06	0.49	−0.44
23	0.56	0.35	0.47	0.02	0.48	−0.45
24	0.56	0.56	0.47	−0.005	0.48	−0.38

We postulate, then, that the decadal shifts in tropical Pacific climate in the last century may possibly be operating with the basic physics of internal tropical variability as modeled by ZC.

Given that the temporal pattern of observed shifts can be reproduced by the ZC model, our objective is to assess their predictability in the presence of initial condition noise. For each of the 72 model analog series, a suite of 100 forecasts was performed with the ZC model. Each ensemble member was initialized in the month of January, 5 yr prior to the shift point and integrated forward for 20 yr. Since we are forecasting from a state along a known ZC model trajectory, the initialization procedure is a straightforward insertion of the model state. The initial condition of each member of the ensemble differed only by the addition of a perturbation to the model SST field. The perturbation at each grid point was sampled randomly from a zero mean uniform distribution. The ZC model's SST standard deviation at each grid point was used to determine the standard deviation of the perturbation to the corresponding grid point.

This generates ensemble initial conditions that deviate from the true initial conditions by a spatially uncorrelated pattern. Thus, the model must glean its predictability from the large-scale, coherent ocean/atmosphere structures that are not destroyed by the application of noise.

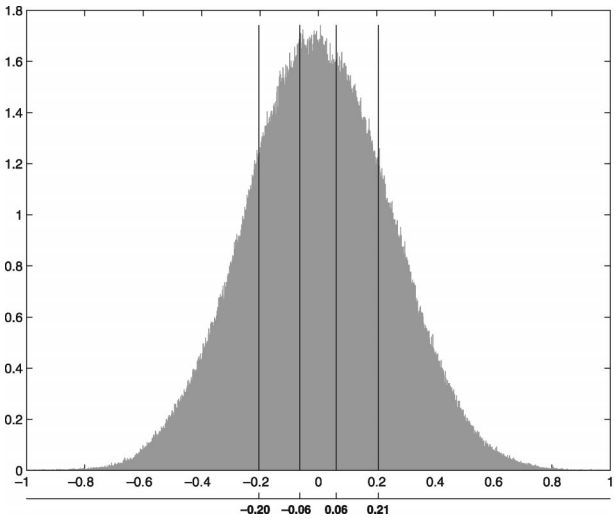

FIG. 2. Distribution of shifts in means of adjacent 15-yr segments of Niño-3 SSTA (in °C) from 150 000-yr integration of ZC model. Quintiles marked in solid black lines.

We present the predictability in two ways: 1) as a function of the sense of the shift (i.e., *warm*, *neutral*, or *cold* shift) and 2) as a function of the mean SST anomaly in the Niño-3 area in the 10-yr period leading up to the forecast initialization. The latter is based on the pragmatic notion that in an operational forecast system the most useful classification of predictability is based on the available observations, that is, the current and past state of the system.

For each of the 100 perturbed initial states it is determined whether the model could properly forecast the shift. In order to quantify the definition of a shift in the model space, we consider a probability distribution of differences in the mean of sequential 15-yr segments. These are derived, again, from ZC-Long. This distribution is divided into quintiles, with equal likelihood of occurrence in each bin (Fig. 2).

For the 24 warm shift analogs, the forecast is ''correct'' if the shift is in the fifth (highest) quintile, ''weakly correct'' if it is off by only one quintile (i.e., in the fourth quintile), and ''wrong'' if it is off by more than one quintile. Similar definitions apply to cold and neutral shifts as illustrated in Fig. 3.

Table 2 (left side) shows the relative frequencies of correct, weakly correct, and wrong forecasts. These are the raw counts divided by the total sample size, expressed as a percentage. The results are presented as a function of the sense of the shift (either warm, neutral, or cold). Warm shifts are shown to be predictable almost 60% of the time, far more than either cold or neutral shifts.

Next, we present the predictability as a function of the initial decadal mean SST anomaly. Every 10-yr period in ZC-Long is classified as either a ''warm'' ''cold,'' or ''neutral'' decade, with these classes defined such that there is equal probability of being in each of

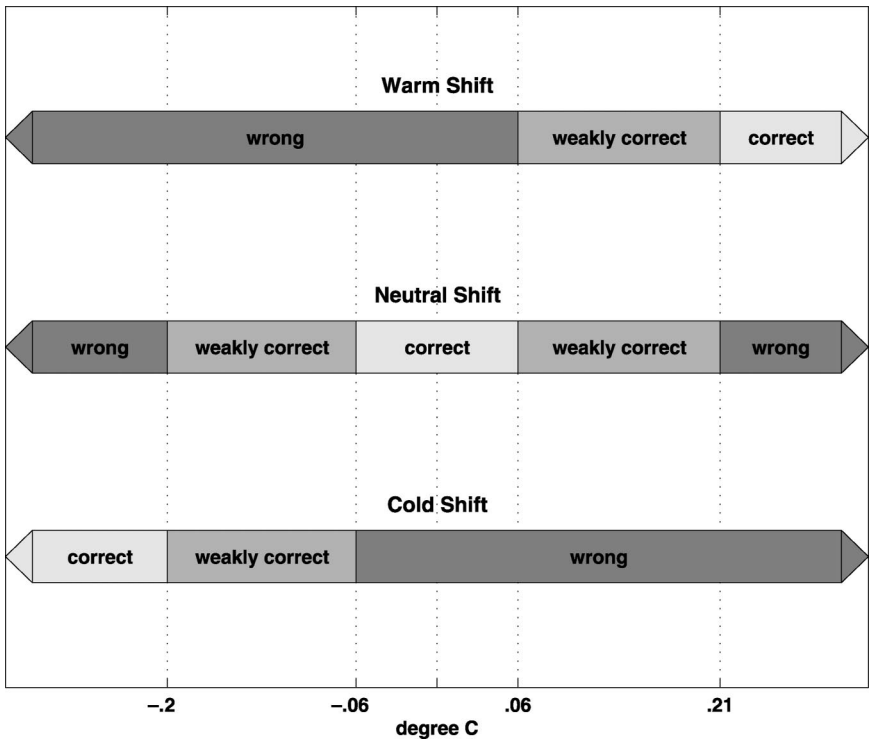

FIG. 3. For warm, neutral, and cold shifting analog series, the range of shift sizes that are designated as correct, weakly correct, and wrong.

TABLE 2. Performance of the dynamical model and two naive forecasting strategies presented as a function of the sense of the shift (warm, neutral, or cold). Results for the dynamical model are based on 100 member ensembles for each of the 72 analog series (24 each of warm, neutral, and cold shifts). Ensembles of size 500 000 were used for the naive forecasts.

				Naive reference forecasts					
	ZC dynamical forecasts			ZC-Long			AR (2)		
	Correct (%)	Weak (%)	Wrong (%)	Correct (%)	Weak (%)	Wrong (%)	Correct (%)	Weak (%)	Wrong (%)
Warm shift	59	23	18	42	26	32	47	16	37
Neutral shift	21	45	34	18	39	43	14	30	56
Cold shift	41	23	36	30	22	48	34	14	52

these states. Figure 4 shows the distribution of 10-yr mean Niño-3 SST anomaly values from ZC-Long. Terciles have been marked with solid black lines. The small bias in the model SST fields has been removed. Any decade with a mean less than −0.11°C is by definition cold, between −0.11° and 0.10°C is deemed neutral, and greater than 0.10°C is defined as warm. Each of the 72 analogs are sorted by their initial 10-yr state (warm, neutral, or cold).

Table 3 (left side) shows the relative frequencies of correct, weakly correct, and wrong forecasts as a function of the 10-yr mean SST anomaly leading up to the initialization. Forecasts that were initialized during warm and cold decades are shown to be correct 46% and 43% of the time, respectively, while neutral starts are correct only about one-third of the time. The near symmetry of this result is worth noting. It can be interpreted as the model's tendency toward greater long-term stability (to perturbations) during anomalously warm or cold decades. Alternatively, decades with a mean closer to zero can be considered to be more unstable to perturbations (on decadal time scales) and hence more susceptible to errors in forecast initialization.

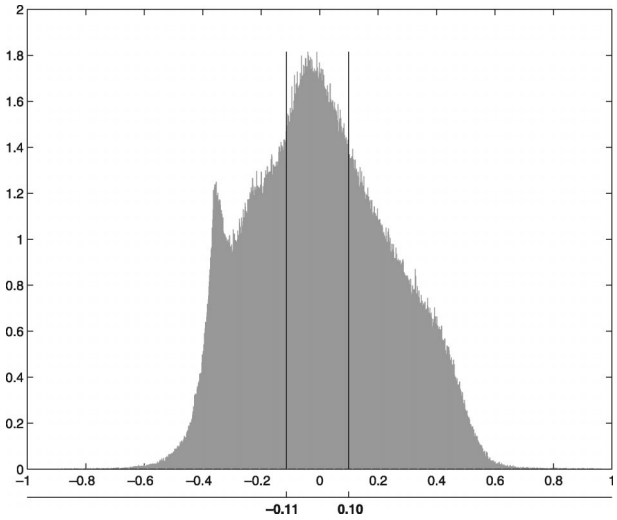

FIG. 4. Distribution of 10-yr means of Niño-3 SSTA (in °C) from ZC-Long (150 000-yr integration of ZC model). Terciles marked in solid black lines.

4. Comparison to naive forecast strategies

When assessing forecast performance, it is common to think in terms of *relative* accuracy, or accuracy compared to some reference forecast. We have chosen two empirical strategies, which we call our ''naive forecasts.'' They are each variations on the following idea: If we have no meaningful understanding of the dynamics of the system, then our best guess is to forecast from an empirical distribution of possible model states. This means that any skill that the naive forecasts may have will stem from having anomalous *initial states.* Statistically extreme initial states will most often result in an appreciable shift in the decadal means because the naive forecast always tends toward a statistical medium (the mode of the distribution). We would not wish to impute skill to the dynamical forecasts if all they are able to capture is the tendency to shift away from the extreme states.

These ''naive'' schemes will be used as null hypotheses against which to measure the skill of the ZC dynamical forecasts. As in the dynamical forecasts, we initialize each forecast in the month of January, 5 yr prior to the shift point. The following two subsections describe each of the naive forecasting strategies.

a. Null 1: Forecasting from a decadal distribution of ZC-Long

From ZC-Long, we constructed a population **X**, the elements of which are given by the following summations:

$$\mathbf{X}(j) = -\frac{1}{180}\left(\sum_{i=j}^{j+59} x_i\right) + \frac{1}{180}\left(\sum_{i=j+60}^{j+239} x_i\right). \qquad (1)$$

Here, x_i are the sequential values of ZC-Long and j is indexed through them. The second term in (1) represents the time average of a 15-yr segment of the ZC-Long series. The first term is the weighted sum of the preceding 5 yr in ZC-Long. We make our naive forecasts from the distribution of **X**.

For each of the 72 analog time series, we calculated the statistic $Y = -(1/180)(\Sigma_{i=1}^{120} y_i)$, where y_i are the monthly elements of the analog time series for the 10 yr prior to the forecast initialization point. Adding the Y value to a sample from **X** gives the difference in the

TABLE 3. As in Table 2 except that performance results are presented as a function of the SST in the decade of initialization. Results for the dynamical model are based on 100-member ensembles for each of the 72 analog series. Ensembles of size 500 000 were used for the naive forecasts. There were 17, 18, and 37 warm, neutral, and cold initial starts, respectively.

				Naive reference forecasts					
	ZC dynamical forecasts			ZC-Long			AR (2)		
	Correct (%)	Weak (%)	Wrong (%)	Correct (%)	Weak (%)	Wrong (%)	Correct (%)	Weak (%)	Wrong (%)
Warm start	46	24	30	37	23	40	37	17	46
Neutral start	32	31	37	19	28	53	22	21	57
Cold start	43	31	26	35	32	33	33	23	44

time average of the second and first 15-yr segments, that is, the shift size. A schematic illustration of this is shown in Fig. 5.

To get an ensemble of shift sizes for each analog, we generated 500 000 random samples from the population **X** and added them to the Y value. This procedure is equivalent to forecasting the 20 yr after the initialization point by randomly choosing 20-yr segments from ZC-Long and then computing the shift size by taking the difference in means between the second and first 15-yr segments. This method of forecasting is meant to capture the statistical behavior of the model's *decadal mean* states. As such, it contains information about any regime-type behavior intrinsic to the model.

The prediction skill is assessed in a manner identical to that described in section 3. Tables 2 and 3 show the relative frequencies of correct, weakly correct, and wrong forecasts as a function of the state of the decade preceding the shift and the sense of the shift.

b. Null 2: Forecasting with a monthly AR(2) model

Next we construct a second-order autoregressive [AR(2)] approximation of the ZC model using values from ZC-Long. We use AR(2) as our null hypothesis rather than the more usual AR(1) because an AR(1) model cannot capture an oscillation; unlike ENSO, it would lack a spectral peak. The seasonality of the model is taken into account by constructing separate AR(2) coefficients for each calendar month. The size of the noise term is determined such that the variance of the AR(2) model is equal to the variance of the ZC model. The mean of the AR(2) model is also adjusted to be equal to the mean of the ZC model.

The monthly AR(2) model is fundamentally different from the statistical forecast presented in the preceding subsection because it is designed to capture the interannual variability of the model. Any regimelike behavior of the AR(2) model results from the integration of continuously applied white noise.

This AR(2) model is used to forecast for 20 yr after the initialization point in each of the analog time series. The uniqueness of each AR(2) forecast results from generating a different noise series for each ensemble member. The shift size for each of the 500 000 ensemble members is calculated as in the previous section. Prediction skill is assessed as in section 3. Tables 2 and 3 summarize the results.

5. Quantifying the ZC model performance in relation to the naive forecasts

We choose the commonly used ranked probability score (RPS; Epstein 1969) as a single metric to assess the forecast skill of each of our methods. The RPS is a type of squared error score that is sensitive to distance, where the score penalty for incorrect forecast probabilities increases for categories further from the actual event outcome. This is achieved by computing the squared errors with respect to the cumulative probabilities of each category. In terms of the categorical probabilities for the forecasts and "true" outcome (f_j and o_j), the RPS can be written:

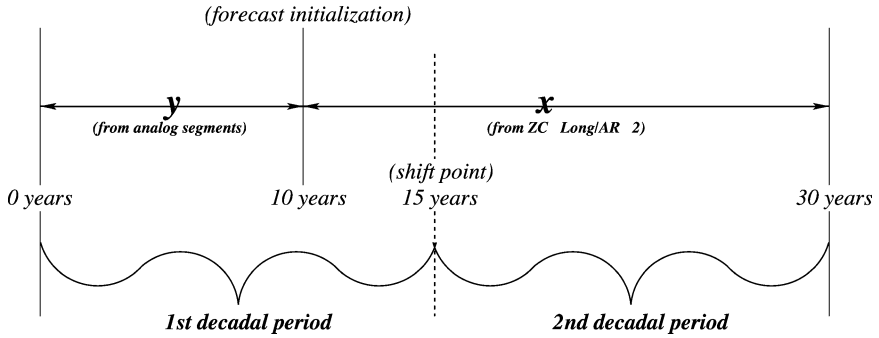

FIG. 5. Schematic of naive forecasting strategies.

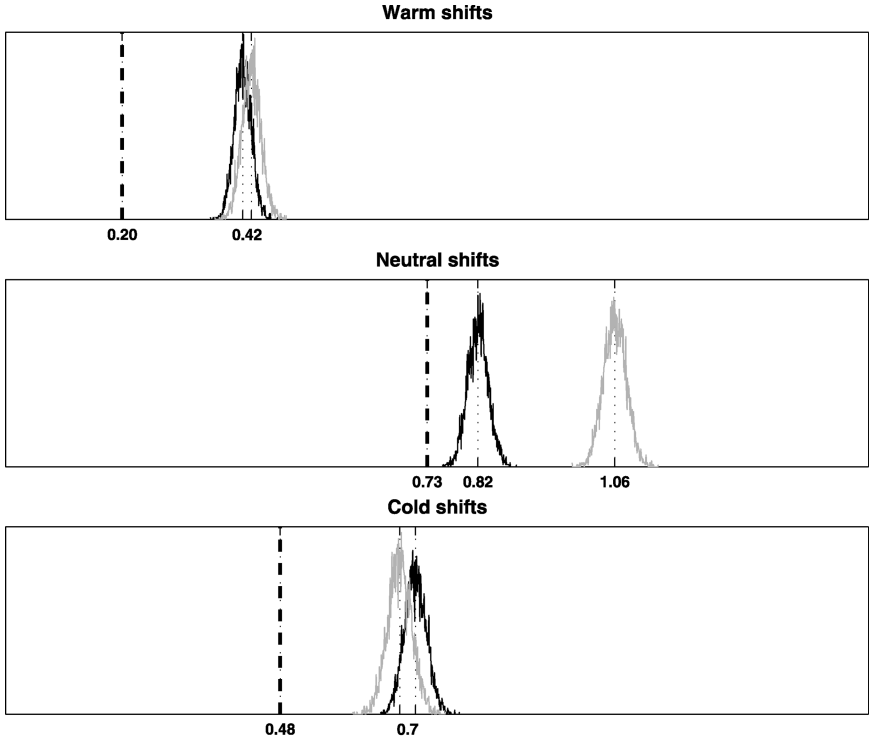

FIG. 6. Bootstrapped distribution of ranked probability score (RPS) for ZC-Long (black) and AR(2) (gray) naive forecasting stategy, presented as a function of the sense of the shift. Distribution is based on 5000 RPS values, each computed from a 100 member ensemble of forecasts. The ZC model dynamical forecast RPS is marked with a bold, dashed black line.

$$\text{RPS} = \sum_{m=1}^{J} \left[\left(\sum_{j=1}^{m} f_j \right) - \left(\sum_{j=1}^{m} o_j \right) \right]^2, \qquad (2)$$

where $J = 3$ is the number of forecast categories, [''correct'' ''weakly correct'' ''incorrect'']. The true outcome (o_j) is always correct and is equal to [1 0 0] in all cases. The internal summations in (2) represent the cumulative probabilities. Note that a perfect forecast has an RPS of 0, and the worst possible score is ($J - 1$), or 2.

As a means of assessing how likely it would be for the naive forecast skill scores to differ from the dynamical forecast skill score by chance alone, we ''bootstrap'' distributions of RPS values for each of our naive forecasting strategies. For each of the 72 initializations, 100 member ensembles of the null forecasts were remade 5000 times (for comparison to the 100 dynamical ensemble members). The RPS was calculated for each set of 100. The distributions for forecasts of warm, cold, and neutral shifts are plotted in Fig. 6. The distributions of forecasts initialized in warm, neutral, and cold decades are shown in Fig. 7. None of the 5000 RPS values for the naive forecasts fall below the dynamical forecast RPS value. This suggests that the extent to which the skill of the dynamical forecasts outperforms both of our statistical naive forecasting strategies cannot be attributed to chance.

A notable feature of Fig. 6 is that for neutral shifts the AR(2) model does appreciably worse than the ZC-Long statistical forecasts. To understand this feature, it is necessary to consider the *starting state* of the majority of the neutral shifts. Seventeen of the 24 neutral forecasts start out in a ''cold decade.'' In order for their forecasts to be deemed correct, they would have had to stay within 0.06°C of the original state, which would mean remaining in a cold state for 20 yr. It would be very unusual for an AR(2) model to do this: it exhibits much less regimelike behavior than the dynamical model (and thus the ZC-Long statistical forecast). A distribution of 10-yr means for the AR(2) model would be more narrow than that of the ZC model. This discrepancy is also evident in the ''cold starts'' in Fig. 7.

6. Results and conclusions

The ZC dynamical model outperforms both naive forecasting strategies. This is evident from the relative frequency of correct shifts (Tables 2 and 3) and from the ranked probability score values in Figs. 6 and 7. This suggests that the model has some predictability beyond a simple tendency to drift toward its own gross statistical behavior. Warm shifts forecasted with the ZC dynamical model have the greatest predictability. However even the naive forecasts perform well for warm shifts. Starting decades that are classified as warm and

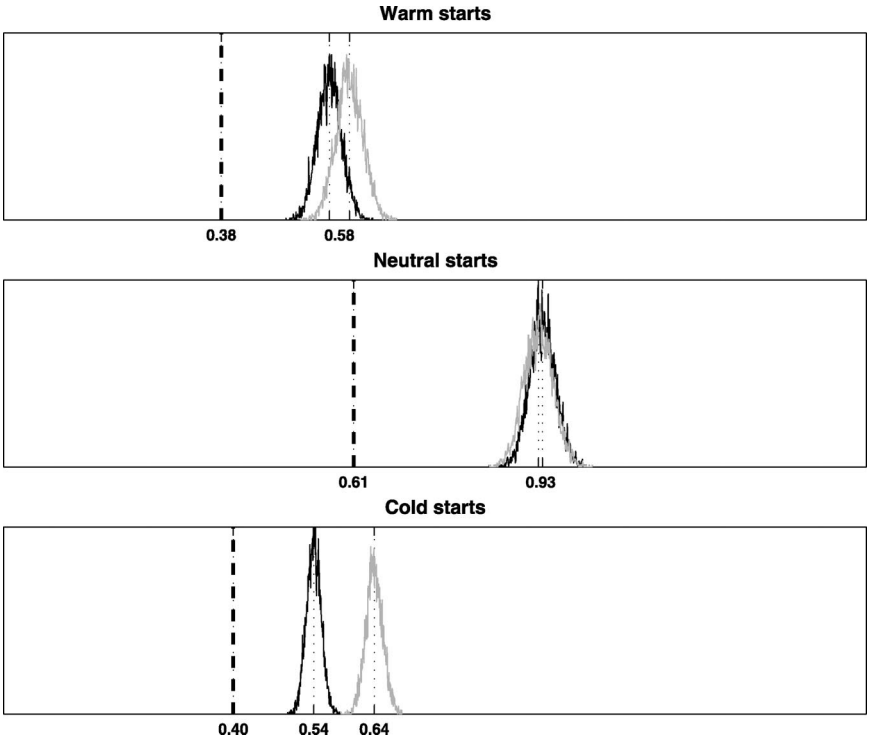

FIG. 7. Bootstrapped distribution of RPS for ZC-Long (black) and AR-2 (gray) naive forecasting stategy, presented as a function of the mean SST in the decade of initialization. Distribution is based on 5000 RPS values, each computed from a 100-member ensemble of forecasts. The ZC model dynamical forecast RPS is marked with a bold, dashed black line.

cold have greater predictability than neutral starts. The dynamical model forecasts initiated in neutral decades actually produce a ''wrong'' shift more often than a ''weak'' or ''correct'' shift, although not as often as the naive forecasts.

The results presented here suggest that the absolute predictability of this dynamical model is marginal. However it is intriguing to see that the ZC model consistently outperforms the naive forecasts, leading us to speculate that the state of the Tropics 5 yr prior to a shift in the PDV may contain the informational seed that drives the shift a half decade later. The extent to which a tropical-only model can mimic observed decadal shifts in tropical Pacific climate lends a modest amount of support to the paradigm of PDV driven from within the Tropics.

The mechanism of decadal variability in the ZC model was investigated by Timmermann and Jin (2002). They argue that decadal modulation of the ENSO cycle in the ZC model results from the nonlinear interaction between the strength of the anomalous zonal SST advection and the dynamical adjustment time of the thermocline to wind-forced Rossby waves.

When we discuss the assessment of model *predictability*, it is useful to keep in mind the difference between examining sources of error growth in a model and measuring a model's skill at forecasting reality (i.e., how well the model dynamics are able to reproduce the observations). For predictability, the perfect forecast, or ''truth,'' is a trajectory that the model is capable of reproducing exactly (given the proper initial conditions). The assessment of predictability, in this case, is quantifying the extent to which small errors in the initial conditions can grow in time and eventually cause the model to stray from its true trajectory. The work that we are presenting in this study focuses on this type of predictability assessment. It is one means of testing whether or not there are large-scale, coherent patterns that can evolve consistently, even in the presence of initialization noise.

In the practical case of forecasting reality, we no longer assume that the model is perfect or capable of evolving along the true trajectory. The truth is defined by the natural system that the model dynamics were designed to emulate. The extent to which the model is able to follow an observed trajectory is the true measure of its skill. Of course the true test of the utility of the ZC model for decadal predictions of tropical climate shifts would be its application to retrospective forecasts (such as retrospectively forecasting the 1976 shift). The primary problem with this undertaking is the lack of reliable oceanic and atmospheric data available to initialize the forecasting model. The fields that *are* available in the early 1970s are analysis products that contain very little observed data. Uncertainty in the initial conditions would plague an interpretation of the results of

a forecast. If it holds true that the sign of the PDV has in fact shifted as of 1998, that shift could turn out to be a reasonable candidate for assessing the ZC model's skill at operational forecasts of decadal climate shifts.

Acknowledgments. This study was supported by the NASA Earth Systems Science graduate fellowship. Additional funding was provided by NSF Grant ATM-9986072 and NOAA Grants UCSIO-CU-02165401-SCF and NA16GP2024. Many thanks (and good luck) to Ben Kerman for his preliminary work on this topic.

REFERENCES

Alexander, M., 1992: The midlatitide atmosphere–ocean interaction during El Niño. Part I: The North Pacific Ocean. *J. Climate,* **5,** 944–958.

——, I. Blade, M. Newman, J. Lanzante, N. Lau, and J. Scott, 2002: The atmospheric bridge: The influence of ENSO teleconnections on air–sea interaction over the global oceans. *J. Climate,* **15,** 2205–2231.

Battisti, D., 1998: Dynamics and thermodynamics of a warming event in a coupled tropical atmosphere–ocean model. *J. Atmos. Sci.,* **45,** 2889–2919.

Chang, P., L. Ji, B. Wang, and T. Li, 1995: Interactions between the seasonal cycle and El Niño–Southern Oscillation in an intermediate coupled ocean–atmosphere model. *J. Atmos. Sci.,* **52,** 2353–2372.

Epstein, E., 1969: A scoring system for probability forecasts of ranked catagories. *J. Appl. Meteor.,* **8,** 985–987.

Graham, N., 1994: Decadal-scale climate variability in the tropical and North Pacific during the 1970s and 1980s: Observations and model results. *Climate Dyn.,* **10,** 135–162.

Gu, D., and S. G. H. Philander, 1997: Interdecadal climate fluctuations that depend on exchanges between the Tropics and the extratropics. *Science,* **275,** 805–807.

Guilderson, T., and D. Schrag, 1998: Abrupt shift in subsurface temperatures in the tropical Pacific associated with changes in El Niño. *Science,* **281,** 240–243.

Hare, S., N. Mantua, and R. Francis, 1999: Inverse production regimes: Alaska and West Coast Pacific salmon. *Fisheries,* **24,** 6–14.

Hazeleger, W., R. Seager, M. A. Cane, and N. H. Naik, 2004: How can tropical Pacific ocean heat transport vary? *J. Phys. Oceanogr.,* **34,** 320–333.

Kaplan, A., M. Cane, Y. Kushnir, A. Clement, M. Blumenthal, and B. Rajagopalan, 1998: Analysis of global sea surface temperature 1856–1991. *J. Geophys. Res.,* **103,** 18 567–18 589.

Karspeck, A., and M. Cane, 2002: Tropical Pacific 1976–77 climate shift in a linear, wind-driven model. *J. Phys. Oceanogr.,* **32,** 2350–2360.

Knutson, T., and S. Manabe, 1998: Model assessment of decadal variability and trends in the tropical Pacific Ocean. *J. Climate,* **11,** 2273–2296.

Latif, M., 1998: Dynamics of interdecadal variability in coupled ocean–atmosphere models. *J. Climate,* **11,** 602–624.

——, and T. P. Barnett, 1996: Decadal climate variability over the North Pacific and North America: Dynamics and predictability. *J. Climate,* **9,** 2407–2423.

Lau, N., 1997: Interactions between global SST anomalies and the midlatitude atmospheric circulation. *Bull. Amer. Meteor. Soc.,* **78,** 21–33.

——, and M. Nath, 1996: The role of the ''atmospheric bridge'' in linking Pacific ENSO events to extratropical SST anomlies. *J. Climate,* **9,** 2036–2057.

Mantua, N., S. Hare, Y. Zhang, J. Wallace, and R. Francis, 1997: A Pacific interdecadal climate oscillation with impacts on salmon production. *Bull. Amer. Meteor. Soc.,* **78,** 1069–1079.

Miller, A., and N. Schneider, 2000: Interdecadal climate regime dynamics in the North Pacific Ocean: Theories, observations and ecosystem impacts. *Progress in Oceanography,* Vol. 47, Pergamon, 355–379.

——, D. Cayan, T. Barnett, N. Graham, and J. Oberhuber, 1994a: Interdecadal variability of the Pacific Ocean: Model response to observed heat flux and wind stress anomalies. *Climate Dyn.,* **9,** 287–302.

——, ——, ——, ——, and ——, 1994b: The 1976–77 climate shift of the Pacific Ocean. *Oceanography,* **7,** 21–26.

Nonaka, M., S. Xie, and J. McCreary, 2002: Decadal variations in the subtropical cells and equatorial pacific SST. *Geophys. Res. Lett.,* **29,** 1116, doi:10.1029/2001GL013717.

Seager, R., A. Karspeck, M. Cane, Y. Kushnir, A. Giannini, A. Kaplan, B. Kerman, and J. Velez, 2004: *Ocean–Atmosphere Interaction and Climate Variability.* Amer. Geophys. Union, in press.

Suarez, M., and P. Schopf, 1988: A delayed oscillator for ENSO. *J. Atmos. Sci.,* **45,** 3283–3287.

Timmermann, A., and F. Jin, 2002: A nonlinear mechanism for decadal El Niño amplitude changes. *Geophys. Res. Lett.,* **29,** 1003, doi:10.1029/2001GL013369.

Trenberth, K., and J. Hurrell, 1994: Decadal atmosphere–ocean variations in the Pacific. *Climate Dyn.,* **9,** 303–319.

Vimont, D., D. Battisti, and A. Hirst, 2001: Footprinting: A seasonal link between the midlatitudes and Tropics. *Geophys. Res. Lett.,* **28,** 3923–3926.

Zebiak, S., and M. Cane, 1987: A model El Niño–Southern Oscillation. *Mon. Wea. Rev.,* **115,** 2262–2278.

Zhang, Y., J. Wallace, and D. Battisti, 1997: ENSO-like decade-to-century scale variability: 1900–93. *J. Climate,* **10,** 1004–1020.